Soil Biology & Biochemistry 53 (2012) 133–141

Contents lists available at SciVerse ScienceDirect

Soil Biology & Biochemistry

journal homepage: www.elsevier.com/locate/soilbio

A theoretical model of C- and N-acquiring exoenzyme activities, which balances microbial demands during decomposition

Daryl L. Moorhead [a,*], Gwenaëlle Lashermes [b], Robert L. Sinsabaugh [c]

[a] Department of Environmental Sciences, University of Toledo, 2801 W. Bancroft St. Toledo, OH 43606-3390, USA
[b] INRA, UMR614 FARE, 2 Esplanade Roland Garros, F-51100 Reims, France
[c] Department of Biology, 1 University of New Mexico, Albuquerque, NM 87131-0001, USA

ARTICLE INFO

Article history:
Received 31 January 2012
Received in revised form
10 May 2012
Accepted 13 May 2012
Available online 2 June 2012

Keywords:
Decomposition
Extracellular enzymes
Model
Ecological stoichiometry
Threshold element ratio (TER)
Overflow metabolism
Carbon use efficiency

ABSTRACT

We developed an Extracellular EnZYme model (EEZY) of decomposition that produces two separate pools of C- and N-acquiring enzymes, that in turn hydrolyze two qualitatively different substrates, one containing only C (e.g., cellulose) and the other containing both C and N (e.g., chitin or protein). Hence, this model approximates the actions of commonly measured indicator enzymes ß-1,4-glucosidase and ß-1,4-N-acetylglucosaminidase (or leucine aminopeptidase) as they hydrolyze cellulose and chitin (or protein), respectively. EEZY provides an analytical solution to the allocation of these two enzymes, which in turn release C and N from the two substrates to maximize microbial growth. Model behaviors were both qualitatively and quantitatively consistent with patterns of litter decay generated by other decomposition models. However, EEZY demonstrated greater sensitivity to the C:N of individual substrate pools in addition to responding to factors directly affecting enzyme activity. Output approximated field observations of extracellular enzyme activities from studies of terrestrial soils, aquatic sediments, freshwater biofilm and plankton communities. Although EEZY is largely a theoretical model, simulated C- and N-acquiring enzyme activities approximated a 1:1 ratio, consistent with the bulk of these field observations, only when the N-containing substrate had a C:N ratio similar to commonly occurring substrates (e.g., proteins or chitin). This result supported the emerging view of the stoichiometry of extracellular enzyme activities from an environmental context, which suggests that a relatively narrow range of microbial C:N, carbon use efficiency and soil/sediment organic matter C:N across ecosystems explains the tendency towards this 1:1 ratio of enzyme activities associated with C- and N-acquisition. Sensitivity analyses indicated that simulated extracellular enzyme activity was most responsive to variations in carbon use efficiency of microorganisms, although kinetic characteristics of enzymes also had significant impacts. Thus EEZY provides a quantitative framework in which to interpret mechanisms underlying empirical patterns of extracellular enzyme activity.

1. Introduction

Decomposer microorganisms obtain their energy and nutrients from dead organic matter by producing hydrolytic and oxidative enzymes that catalyze the extracellular degradation of complex organic molecules (Burns, 1978; Burns and Dick, 2002). It is difficult to quantify the mass of enzymes in environmental samples, but their potential activities can be readily assayed (Sinsabaugh et al., 1997; Marx et al., 2001) and compared to rates and patterns of litter decay (Sinsabaugh, 1994). Recent syntheses indicate that the relative balance in activities of extracellular enzymes responsible for C, N and P acquisition reflect the stoichiometric (balance of elements) and metabolic (energy) needs of microorganisms (Sinsabaugh et al., 2008, 2009, 2010, 2011). Moreover, Sinsabaugh et al. (2009) suggest that a convergence in microbial characteristics (C:N, carbon use efficiency), organic matter chemistry (C:N), and patterns in extracellular enzyme activities reveal a global pattern of the stoichiometry of extracellular enzyme activity across ecosystems. However, few mathematical models have sufficient mechanistic resolution to simulate these patterns (Allison, 2005; Davidson et al., 2012).

The most widely measured enzyme activities generate consumable products from the hydrolysis of the most common pools of detrital organic matter. Cellulose is the largest product of plant production and ß-1,4-glucosidase (ßG), which hydrolyzes glucose from cellobiose and other celloligosaccharides, is the most commonly measured cellulose-degrading enzyme. The largest

* Corresponding author. Tel.: +1 419 530 2017; fax: +1 419 530 4429.
E-mail address: daryl.moorhead@utoledo.edu (D.L. Moorhead).

0038-0717/$ – see front matter © 2012 Elsevier Ltd. All rights reserved.
doi:10.1016/j.soilbio.2012.05.011

organic N sources are proteins and chitins. For protein, leucine aminopeptidase (LAP) hydrolyzes the most abundant protein amino acid from the ends of polypeptides and is the most commonly measured indicator enzyme. For chitin, the most commonly measured indicator enzyme is ß-1,4-*N*-acetylglucosaminidase (NAG), which hydrolyzes *N*-acetylglucosamine from chitobiose and other chito-oligosaccharides (Sinsabaugh, 1994; Sinsabaugh et al., 1997). Although the degradation of polymeric compounds into assimilable substrates usually requires the interactions of many enzymes, the activities of hydrolytic enzymes that target the same classes of compounds are strongly correlated (Sinsabaugh et al., 2011). Because the activities of extracellular enzymes link microbial metabolism to decomposition processes, they provide a uniquely mechanistic insight to biogeochemical cycles (Sinsabaugh et al., 2008, 2010, 2011; Sinsabaugh and Shah, 2011; Marklein and Houlton, 2011). Not surprisingly, more studies of environmental enzymes, decomposition and soil organic matter dynamics couple C and N biogeochemical cycles than any other elements.

Manzoni and Porporato (2009) recently reviewed 250 biogeochemical models and found that few of them described decomposition as a direct product of microbial activity, and even fewer included the activities of extracellular enzymes. The best-known exception was the model developed by Schimel and Weintraub (2003), which includes one pool of extracellular enzymes that hydrolyzes one pool of soil organic matter for use by one pool of microorganisms. It is based on a general, mechanistic model developed by Parnas (1976) that linked microbial C:N stoichiometry (CN_M) to soil organic matter C:N content (CN_S) by carbon use efficiency (CUE; fraction of carbon released from organic matter that is incorporated in biomass), such that decomposition exactly meets microbial C and N demands for growth when $CN_M = CN_S/CUE$. However, Parnas (1976) calculated decay rate with a typical Michaelis–Menten equation of substrate-saturation, i.e., substrate pool size regulated the rate. In contrast, Schimel and Weintraub (2003) used a Michaelis–Menten equation of enzyme-saturation, which regulated decay rate by the amount of extracellular enzyme present. This was a substantial improvement over an earlier, possibly the first, enzyme-based decomposition model (Sinsabaugh and Moorhead, 1995), which calculated decay rate as a first-order function of C-acquiring enzyme activity. However, neither of these two enzyme-based models included more than one pool of enzymes, so that model output could not be compared to empirical observations of relative C- versus N-acquiring enzyme activities (Sinsabaugh, 1994; Sinsabaugh and Moorhead, 1994).

Our primary objective in the present study was to develop a decomposition model that used two specific enzymes to gain C and N from organic matter to meet microbial energy and nutrient requirements. This is the minimum model complexity that can be used to explore the factors responsible for balancing the activities of these enzymes reported from experimental observations. We also wanted a parsimonious approach that was yet sufficient to capture these relationships. To this end, we integrated key methods used by Parnas (1976), Sinsabaugh and Moorhead (1994, 1995) and Schimel and Weintraub (2003) to model the growth and metabolism of a microbial community, and the production of two distinct kinds of enzymes, one that degrades organic molecules containing both C and N (e.g., chitin or protein) and another that degrades molecules containing C but not N (e.g., cellulose). These are the two most common elements included in decomposition models (Manzoni and Porporato, 2009) and enzymes associated with their acquisition are among the most commonly assayed in field studies (Sinsabaugh et al., 2008, 2010, 2011). We then used this model of Extracellular EnZYme (EEZY) activities to generate patterns of enzyme production and activity in response to variations in soil organic matter chemistry, to compare with recent syntheses of field data (Sinsabaugh et al., 2009, 2010, 2011; Sinsabaugh and Shah, 2011). Finally, we conducted a sensitivity analysis to determine the relative importance of variation in key model parameters that represent key features of microbial C and N demands, and kinetics of enzymes responsible for C and N acquisition.

2. Modeling approach

EEZY included six pools of organic carbon: (1) a carbon- + nitrogen substrate (C_1), hydrolyzed by (2) an extracellular pool of enzymes (E_{C1}), (3) a carbon-only substrate (C_2), hydrolyzed by (4) another pool of enzymes (E_{C2}), which together produce a pool of (5) dissolved organic carbon (DOC) that was consumed by (6) microorganisms (B_C) (Fig. 1). Although the model equations are provided in Appendix 1, we present herein those that define the novel feature of EEZY. At the core of our model is the "reverse" Michaelis–Menten equation described by Schimel and Weintraub (2003). They coined this term because this equation estimates

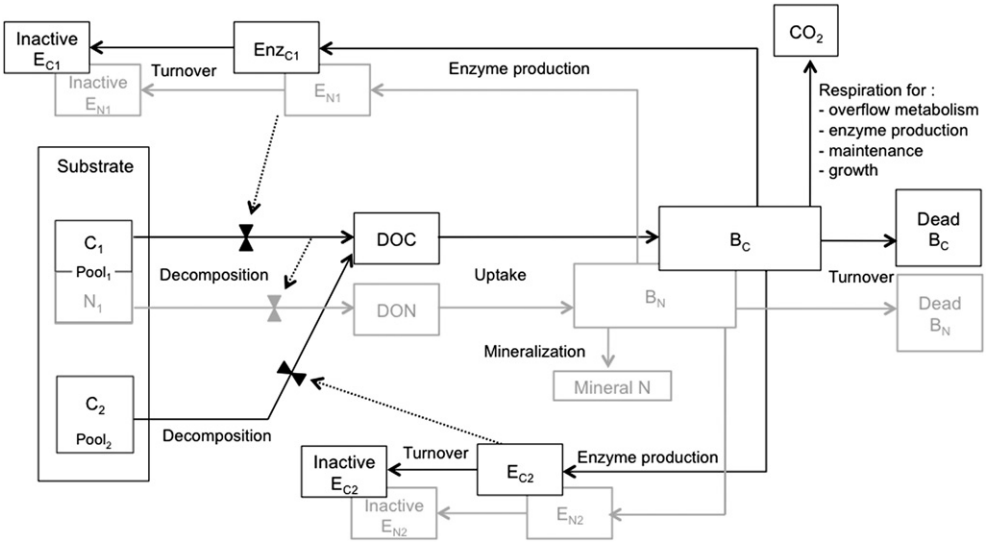

Fig. 1. Carbon (black lines) and nitrogen (gray lines) flow diagram for the EcoEnZYme model (EEZY).

reaction rate as a function of enzyme pool size rather than substrate pool size used in most applications of the Michaelis–Menten function (e.g., Parnas, 1976; Moorhead and Sinsabaugh, 2006; Allison et al., 2010; Davidson et al., 2012):

$$dC_1/dt = -k_d \cdot \alpha \cdot E_{CT}/(K + \alpha \cdot E_{CT}) \quad (1)$$

$$dC_2/dt = -k_d \cdot (1-\alpha) \cdot E_{CT}/(K + (1-\alpha) \cdot E_{CT}) \quad (2)$$

where k_d is the maximum rate of decay for soil organic carbon pools, C_1 and C_2. E_{CT} is the total C in both enzyme pools, K is the half-saturation coefficient for enzyme activity, and α is the fraction of the total enzyme pool that specifically hydrolyzes C_1 (i.e., E_{C1}). The novel feature of EEZY is that we estimate the allocation of the total enzyme pool between two pools of enzymes based on a reverse Michaelis–Menten function. We assume that microorganisms seek C and N from the two C pools in the proportion that exactly satisfies microbial C:N stoichiometry, given carbon use efficiency:

$$CN_M = CUE \cdot (dC_1/dt + dC_2/dt)/((dC_1/dt)/CN_1) \quad (3)$$

where CN_1 is the C:N ratio of C_1. The numerator of this equation estimates total carbon available for microbial growth and enzyme production by multiplying the C released from the decomposition of both substrate pools by CUE. The denominator estimates nitrogen available to support microbial growth and enzyme production by dividing the decomposition of the substrate containing N by its C:N ratio. With this equation, the relative decay rates of the two substrates can be determined by setting the ratio of C and N made available from decomposition equal to the C:N ratio of microbial biomass. We assumed that N-use efficiency was 100% and that CUE was the same for both substrates. We also assumed that the C:N ratio of enzymes (CN_E) was the same as the C:N ratio of microbial biomass (Table 1). The value of α representing the allocation of enzymes necessary to generate this balance of C and N from the decomposition of the two, substrate pools was determined by substituting Eqs. (1) and (2) for dC_1/dt and dC_2/dt in Eq. (3) and simply reorganizing the expanded equation (Appendix 1). Because values of CUE, k_d and K are likely to vary between substrates and enzymes, we then expanded this allocation scheme by adding unique values of k_d and CUE for each of the two substrates and unique values of K for each of the two enzymes in Eqs. (1) and (2). We again estimated α by substituting the modified Eqs. (1) and (2) for dC_1/dt and dC_2/dt in Eq. (3). This second, more complex allocation scheme, permitted an analysis of the importance of variations in these model parameters.

Nitrogen flows balanced C flows in this model, given fixed C:N ratios of donor and recipient pools, and CUE. If the decomposition of C_1 released more N from N_1 than was needed to meet the microbial growth requirement (Eq. (3)), the excess was mineralized and added to the mineral N pool (Fig. 1). For the sake of simplicity, we did not include the immobilization of mineral N into microbial biomass.

The model has a daily time step and all DOC and DON produced by decomposition is taken up by the microbial pool each iteration. It is a steady-state model, so losses from DOC and DON pools due to decomposition were replaced daily. Total enzyme production is assumed to be a fraction of DOC and DON uptake, allocated before other allocations to biomass growth or respiration (Sinsabaugh and Moorhead, 1995; Schimel and Weintraub, 2003). Microbial growth is a fraction of the uptake from the DOC pool minus the allocation to enzyme production. Respiration includes amounts associated with enzyme and biomass production, and a maintenance fraction of the standing biomass per day (R_M). Maintenance respiration has many potential components (Van Bodegom, 2007) but we use it herein as respiration that is not associated with growth. We included another feature of the Schimel and Weintraub (2003) model by allocating to respiratory overflow metabolism (R_O) any carbon released from substrates in excess of microbial need, as may occur when substrates are C-rich and N-poor. Overflow metabolism occurs when catabolism is decoupled from growth and is commonly reported in cultured microorganisms (e.g., Santos et al., 2012). However, Schultz and Urban (2008) also reported excess C respired by soil microbial communities with no increase in microbial biomass or enzyme activity. Including this mechanism in EEZY permitted decomposition of N-limited substrates according to the rationale presented above.

2.1. Simulations

We conducted several simulations (Table 2) to explore the behavior of this model. In all but the last set, CN_1 was varied between 5:1 and 25:1 to represent a range of characteristics for plant and microbial compounds; Sterner and Elser (2002) estimated average C:N values of 2.2 for peptidoglycans, 2.6 for nucleic acids, 5.0 for chitin, 6.25 for proteins and 49 for phospholipids. The first two sets of simulations used the same values of k_d, K and CUE (Table 1) for both pools of substrates and enzymes, whereas the next three sets of simulations altered the values of each of these parameters, separately.

Our sensitivity analyses held CN_1 at either 10:1 or 30:1, defining C-limited and N-limited conditions, respectively. In both cases, we used 100 randomly chosen values of $k_{d1,\ 1}$ and CUE_1 driving the decomposition of C_1 from within ±10% of the values given in Table 1, to evaluate the sensitivity of model behavior to

Table 1
Initial state variables and parameters used in the EEZY model.

	Factor	Value	Explanation, units
Variables	B_C	1	Microbial biomass C, mg C
	B_N	0.14	Microbial biomass N, mg N
	DOC	0	Dissolved organic carbon, mg C
	DON	0	Dissolved organic N, mg N
	E_{CT}	0.02	C content of total enzyme pool, mg C
	E_{NT}	2.8e−3	N content of total enzyme, mg N
	N_I	0	Inorganic N pool, mg N
	C_1	500	C in substrate pool 1, mg C
	C_2	500	C in substrate pool 2, mg C
	N_1	100	N in substrate pool 1, mg N
Parameters	CN_M	7.16	C:N ratio of biomass, mg C/mg N
	CN_E	7.16	C:N ratio of enzymes, mg C/mg N
	CN_1	5	C:N ratio of C_1, mg C/mg N
	K_N	0.05	Enzyme turnover coefficient, d^{-1}
	k_d	1	Substrate decay rate coefficient, d^{-1}
	K_E	0.05	C-uptake allocated to enzymes, unitless
	K	0.3	Enzyme half-saturation constant, mg C
	K_M	0.01	Maintenance respiration coefficient, d^{-1}
	K_T	0.012	Biomass turnover coefficient, d^{-1}
	CUE	0.5	Substrate C-use efficiency, unitless

Table 2
Simulation scenarios; $k_{d2} = 1.0$, $K_2 = 0.3$ and $CUE_2 = 0.5$ in all scenarios.

Scenario	CN_1	C_1	C_2	k_{d1}	K_1	CUE_1
1	2.5–35	1000	0	1	0.3	0.5
2	2.5–35	500	500	1	0.3	0.5
3	2.5–35	500	500	1	0.3	0.4
4	2.5–35	500	500	1	0.2	0.5
5	2.5–35	500	500	0.8	0.3	0.5
6	10	500	500	1 ± 0.1	0.3 ± 0.03	0.5 ± 0.05
7	30	500	500	1 ± 0.1	0.3 ± 0.03	0.5 ± 0.05

simultaneous variations in parameter values. Three-way ANOVAs were used to evaluate the contributions of variations in k_d, K and CUE to equilibrium values of microbial biomass (B_C), N-mineralization (N_m), overflow metabolism (R_O) and enzyme allocation (α). Type-II sums of squares were interpreted to represent the relative contributions of each parameter to each model result (Moorhead and Sinsabaugh, 2006).

All of the above simulations used a total pool of 1000 mg soil organic carbon. The C_2 pool was set to zero in the first set of simulations, collapsing EEZY to a one-pool model for comparison to Schimel and Weintraub (2003). All of the other simulations divided the C pool into two pools of 500 mg C.

3. Results

3.1. One substrate pool

When the total amount of C (1000 mg) was allocated only to C_1 and CN_1 varied between 5 and 25, the resulting patterns of equilibrium values for microbial biomass (B_C; mg C), overflow respiration (R_O; mg C/d) and N-mineralization rate (N_m; mg N/d) tracked the behavior of the Schimel and Weintraub (2003) model (Fig. 2a),

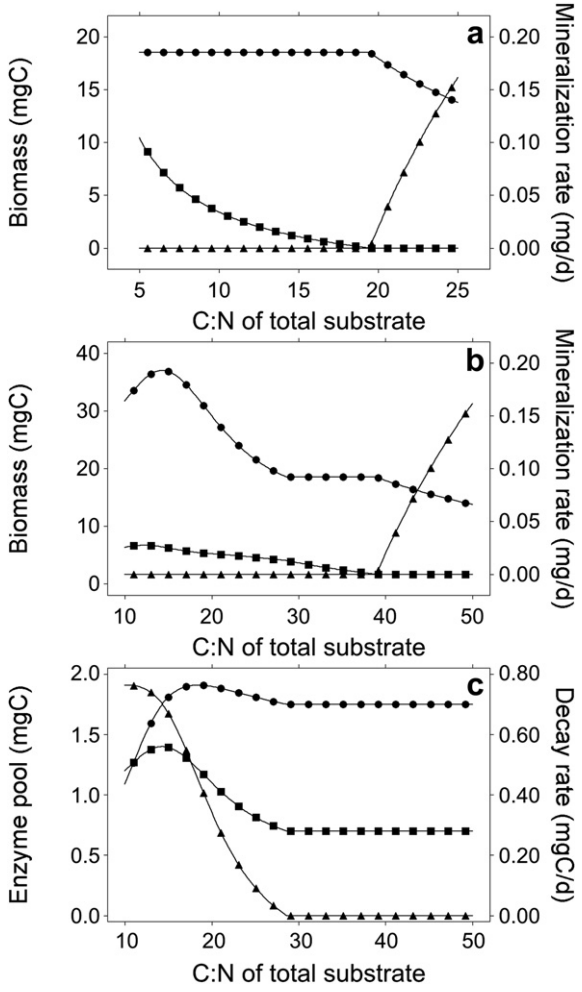

Fig. 2. a. Microbial biomass (circles, mg C), overflow respiration (squares, mg C/d) and the N mineralization (triangles; mg N/d) vs. substrate C:N, when $C_2 = 0$; b. microbial biomass (circles, mg C), overflow respiration (triangles, mg C/d) and the N mineralization (squares; mg N/d) vs. substrate C:N, when $C_2 = C_1$; c. C-flux rates (mg C/d) for decay of C_1 (circles; mg C/d), C_2 (triangles; mg C/d), and total enzyme pool size (squares; mg C), vs. substrate C:N, when $C_2 = C_1$.

albeit at lower values of CN_S because we used a higher value of CN_E (7.16 in EEZY vs. 3 by Schimel and Weintraub, 2003) and did not include mineral N immobilization by biomass. This increase in CN_E reduced the amount of N required for enzyme production in EEZY and thus altered the apparent, simulated threshold element ratio (TER_{CN}; Sterner and Elser, 2002). The TER_{CN} is defined as the resource ratio for C and N (CN_S) at which control of decomposition switches from energy supply (C) to nutrient supply (N). As simulations exceed this ratio, microbial biomass declines, net N-mineralization ceases and overflow respiration starts. The value of TER_{CN} was 19 in EEZY versus 31 by Schimel and Weintraub (2003). However, the behavior of the Schimel and Weintraub (2003) model matches EEZY exactly when CN_E in their model is increased to 7.16 and mineral N is not immobilized (not shown). Thus our two-substrate model behaves the same with one pool of soil organic matter as the single-substrate model of Schimel and Weintraub (2003), by allocating all enzyme biomass to E_{C1}, i.e., $\alpha = 1$.

3.2. Two substrate pools

Adding a second substrate pool to the model produced several changes in model behavior (Fig. 2b). First TER_{CN} increased to about 39 (CN_S). This coincides with a CN_1 ca. 19 and demonstrates how TER_{CN} may vary with more subtle aspects of substrate chemistry than simple bulk measures of element ratios. Biomass also became more variable, reaching a peak of 37 mg C that was twice the maximum value of the first simulations (18.5 mg C). This peak occurred at a CN_1 of about 7:16, which was the same as CN_M, and was coincident with an overall substrate CN_S of about CN_M/CUE = 14. This peak in microbial biomass also corresponded to the peak litter decay rate, which occurred slightly after the maximum decay rate for C_2 and slightly before the maximum decay rate for C_1 (Fig. 2c). Decay rates are driven by enzyme pool sizes (Eqs. (1)–(3)), so that maximum biomass and decomposition coincided with the maximum size (ca. 1.40 mg C) of the total enzyme pool (Fig. 2c). At this point $\alpha = 0.5$, which means that the allocation of the two enzymes was the same for both pools. As CN_S increased above this optimum, α increased and the biomass, decomposition and total enzyme pool decreased.

3.3. Varying CUE, k_d and K

Altering values of CUE, k_d and K controlling the decomposition of substrate C_1 changed some resource thresholds for and magnitudes of model behavior but overall patterns remained similar among all simulations using two substrates. First, reducing the half-saturation coefficient of the enzyme activity (K) degrading substrate C_1 from 0.3 to 0.2 produced a slightly higher peak biomass of 40 mg C (Fig. 3a), coinciding with a slightly greater CN_S of 15 ($CN_1 = 7.51$). The maximum size of the total enzyme pool (E_{CT}) increased slightly from 1.40 to 1.51 mg C, but the value of TER_{CN} remained the same at $CN_S = 39$. Values of α were lower (Fig. 3b) and rates of N-mineralization were higher at all values of $CN_S < TER_{CN}$ (Fig. 3b). Values of R_O also were higher when $CN_s > TER_{CN}$ (not shown).

Next, decreasing the maximum rate of decay for C_1 (k_{d1}) from 1.0 to 0.8 had the opposite effect on model behavior. Peak biomass declined to 32 mg C (Fig. 3a), which occurred at a lower CN_S of 12 ($CN_1 = 6.16$), and the maximum size of the enzyme pool fell to 1.20 mg C. Values of α increased (Fig. 3b) and rates of N-mineralization decreased (Fig. 3c) for all $CN_s < TER_{CN}$. Values of R_O also were lower when $CN_S > TER_{CN}$. However, the value of TER_{CN} was unchanged at $CN_S = 39$.

Finally, reducing CUE for substrate C_1 from 0.5 to 0.4 decreased peak biomass to 34 mg C (Fig. 3a), which occurred at a CN_S of 16

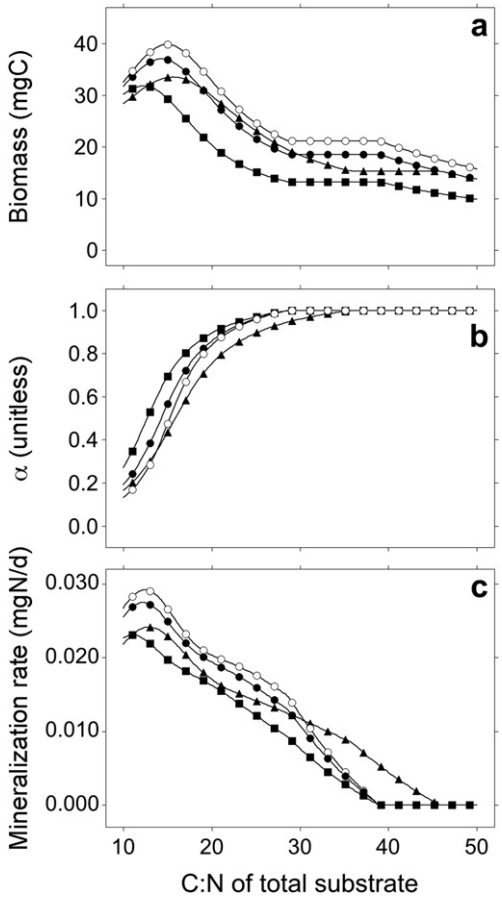

Fig. 3. a. Microbial biomass (mg C), b. ratio of enzyme pool sizes (α, dimensionless), c. N mineralization (mg N/d) when $C_2 = C_1$; baseline parameters (filled circles), reduction in CUE_1 (triangles), reduction in k_{d1} (squares) and reduction in $_1$ (open circles).

($CN_1 = 7.81$). The value of TER_{CN} was increased to $CN_S = 46$ ($CN_1 = 23$), the maximum total size of the enzyme pool fell slightly to 1.38 mg C, α decreased at all values of $CN_S < TER_{CN}$ (Fig. 3b), and R_O was lower when $CN_s > TER_{CN}$. However, due to the increase in TER_{CN}, N-mineralization rates were lower for values of $CN_S < 29$ but greater when $29 < CNs < TER_{CN}$ (Fig. 3c).

3.4. Sensitivity analysis

Results of our sensitivity analysis indicated that variations in all model responses were significantly correlated to variations in k_d, at both levels of CN_1 (Table 3). In most cases, model behavior was also significantly related to variations in CUE, but no model responses were directly correlated to variations in K. However, 3-way ANOVA indicated that all three parameters made significant contributions ($P < 0.05$) to variations in all model responses at both levels of CN_1. In both sets of simulations, predicted values of biomass based on the best-fit regression models, were strongly related to observed values (in both cases $N = 100$, $R^2 \geq 0.996$, $P < 0.01$). In most cases, k_d made the largest contribution (Fig. 4), α was most responsive to variations in CUE, and biomass was much more sensitive to CUE when $CN_S > TER_{CN}$.

Table 3
Correlations between variations in peak microbial biomass, N-mineralization rate enzyme allocation (α), and overflow metabolism (R_O) and variations in key model parameters (k_d, K and CUE) controlling decomposition of substrate C_1, $N = 100$ in all cases.

Parameter	$CN_1 < TER_{CN}$			$CN_1 > TER_{CN}$	
	Biomass	N-mineralization	α	Biomass	R_O
k_{d1}	0.961**	0.922**	−0.327*	0.959**	0.715*
K_1	−0.085	−0.049	0.113	−0.134	−0.035
CUE_1	−0.236*	0.232*	0.947**	−0.093	0.591*

*$P < 0.05$.
**$P < 0.01$.

3.5. Patterns of extracellular enzyme activity

The allocation pattern of enzymes (α) showed a slightly sigmoidal relationship to CN_1 for the baseline model (equal value of CUE, k_d and K for both substrates and both enzymes; Fig. 5a). The nonlinear relationship between decomposition rate and size of the responsible enzyme pool creates the shape of this curve. As one enzyme pool exceeds the other, the relative decay per unit of enzyme mass decreases because enzyme pool sizes tend to exceed K values, i.e., Eqs. (1) and (2) are near saturation. This is why EEZY also produced a roughly hyperbolic relationship between ßG/NAG (i.e., dC_2/dt vs. dC_1/dt) and dC_2/dt (Fig. 5b). This latter relationship represents the relative activities of the enzymes in the same way that Sinsabaugh et al. (2009) reported enzyme activities from environmental samples. Randomly varying CUE, k_d and K by ±10% of baseline values (Table 1) given mean CN_1 values of 5, 7, 9 and 11 (also varied by ±10%) generated a scatter of estimated values, very similar to observed variations in relative activities of C and N-acquiring enzymes (Sinsabaugh et al., 2008).

4. Discussion

4.1. General model behavior

The goal of our study was to explore the relationships between extracellular enzyme activities and soil organic matter chemistry with a model that explicitly simulated the production of enzymes by decomposer microorganisms to balance their C and N requirements during decomposition. We found that dividing the organic matter into two, qualitatively different pools (C-only and C + N substrates) and using two, distinct pools of enzymes that were specific to degrading these substrates added many dynamics to earlier, single-enzyme decomposition models (e.g., Sinsabaugh and Moorhead, 1995; Schimel and Weintraub, 2003). In particular,

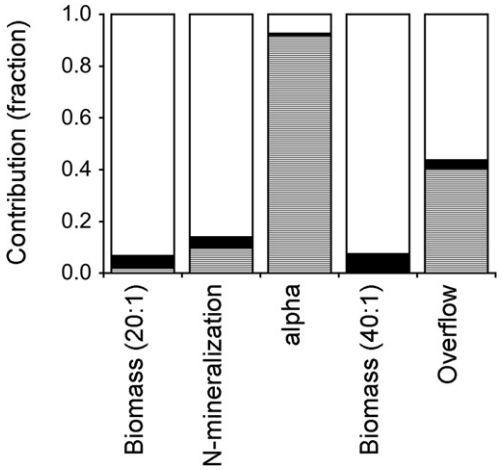

Fig. 4. Relative contribution of variation in each model parameter to explained variation in model behavior; k_{d1} (open bar), K_1 (solid bar), CUE_1 (hatched bar).

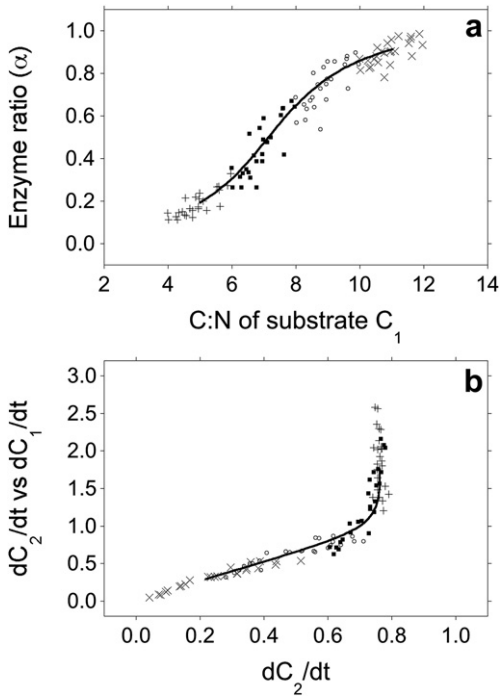

Fig. 5. a. Ratio of enzyme activities (α; dimensionless) for variations in substrate C:N ratio, b. ratio of decay rates for substrates C_2:C_1 versus rate of C_2 decay; baseline parameters (solid line), and with variations in mean ± 10% values of CUE, k_d and K at $CN_1 = 5$ (+), $CN_1 = 7$ (filled squares), $CN_1 = 9$ (open squares), $CN_1 = 11$ (×).

EEZY's behavior was much more variable over the range of substrate C:N values (CN_S) less than TER_{CN} (Fig. 2b,c). When the sole substrate available contained both C and N, peak values of biomass, enzyme production and overall decomposition rate were constant over this range of CN_S (Fig. 2a), determined by the maximum rate of decay (Eq. (1)), with excess N being mineralized. When a second, C-only substrate pool was available, these maxima occurred only when CN_M/CUE approximated CN_1. This optimum was the point at which the balance of C and N released from the two substrates that were decaying at the same rates, matched the C and N demands of microorganisms (Fig. 2c). The allocation of two enzymes to selectively degrade the two substrates permitted a more efficient utilization of N for microbial growth and enzyme production, and reduced simulated N mineralization.

Modifying CUE shifted the optimum balance of C and N release (Eq. (3)), as did changing CN_E, and as would changes in CN_M. Reducing CUE also reduced peak biomass (Fig. 3a) and total enzyme pool sizes, and increased both the value of CN_S corresponding to these peaks and TER_{CN}, because proportionately more C was lost to respiration. The integral role of CUE in the dual control that microbial C and N requirements have on decomposition has been recognized and used in decomposition models since Parnas (1976). However, additional insight was provided by EEZY: reducing CUE for C_1 decreased the relative allocation of enzyme E_{C1} (Fig. 3b), because less C was available to support microbial growth or enzyme production per unit of C_1 decay. Thus allocation schemes for enzyme production *in situ* likely reflect substrate-specific chemical characteristics, substrate-specific microbial characteristics, and enzyme-specific kinetic characteristics, so that observed patterns in extracellular enzyme activity profiles are probably more complicated than suggested by observed relationships between average microbial C and N requirements and average C and N characteristics of decaying organic matter (see below).

Models have only recently included the dynamics of explicit pools of extracellular enzymes and the resulting kinetics of enzyme-mediated decomposition of different substrates (e.g., Allison, 2005). However, adding mechanisms adds potential controls to simulated decomposition. Changes in values of K and k_d affected EEZY dynamics in ways that differed from changes in CUE (Fig. 3). For example, when K for C_1 decreased, the relative rate of C_1 decomposition per unit enzyme E_{C1} increased (Eq. (1)) so that less enzyme E_{C1} was needed to meet the N-demands of microorganisms per unit of C released from C_2. Hence, α declined for all $CN_S < TER_{CN}$ (Fig. 3b) even though TER_{CN} remained constant (only CUE affected TER_{CN}). Biomass and total enzyme pool sizes also increased over this range of CN_S values, and reached peak values at a higher value of CN_S. In contrast, decreasing k_d for C_1 had the opposite effects, reducing biomass and total enzyme pool sizes, and reducing the value of CN_S at which peak values were obtained, because it reduced the decay of C_1 and coupled N_1-release in both absolute amount and relative to potential C_2 decay.

4.2. Patterns of extracellular enzyme activity

In addition to producing plausible patterns of decomposition in response to variations in litter quality and key parameter values, EEZY produced patterns of extracellular enzyme activity (Fig. 5a,b) that added details to an emerging conceptual framework of the stoichiometry of enzyme activities (Sinsabaugh et al., 2009, 2010, 2011; Sinsabaugh and Shah, 2011). In brief, the stoichiometric theory of ecology predicts that TER_{CN} is determined by gross carbon use efficiency (GE_C), gross nitrogen use efficiency (GE_N), and CN_M (Sterner and Elser, 2002; Brown et al., 2004; Frost et al., 2006; Allen and Gillooly, 2009; Doi et al., 2010):

$$GE_C = (GE_N/TER_{CN}) \cdot CN_M \quad (4)$$

in which all sources of respiration are combined into GE_C. In contrast, EEZY calculates respiration from growth and enzyme production, R_M, and R_O separately, but all of these sources of respiration would be included in GE_C. Sinsabaugh et al. (2009) found that the balance of extracellular enzyme activities was related to these same factors:

$$EEA_{CN} = p \cdot (TER_{CN}/CN_M) \text{ and } EEA_{CN} = p \cdot (GE_N/GE_C) \quad (5)$$

where EEA_{CN} is the ratio of C-acquisition to N-acquisition enzyme activity and p is a dimensionless normalization constant. These relationships were based upon observed activities of ß-1,4-glucosidase (ßG), ß-1,4-*N*-acetylglucosaminidase (NAG) and leucine aminopeptidase (LAP) from 445 lotic, 60 lentic and 40 terrestrial sites. The global regression ln(ßG)/ln(NAG + LAP) had a slope of 1.02 and $R^2 = 0.695$ ($P \leq 0.001$, $N = 1434$). Similarly, Sinsabaugh et al. (2010) found slopes of 0.97 ($N = 121$, $R^2 = 0.952$) and 1.06 ($N = 26$, $R^2 = 0.691$) for biofilm and plankton communities, respectively, with differences in slopes related to differences in CN_M between communities. In comparison, EEZY simulations using baseline parameter values (e.g., CUE = 0.5) predicted a 1:1 balance in enzyme activities ($\alpha = 0.5$) at a CN_1 value about equal to CN_M (Fig. 5a), which corresponded to a CN_S of twice the value of CN_M. Variations in CN_1 moved α away from this balance as did variations in CUE, k_d and K (Fig. 5b). Thus a consistent 1:1 value for EEA_{CN} indicates fairly tight constraints on parameter values and C:N ratios associated with these field observations.

Sinsabaugh et al. (2009, 2010) did not report most of the values for parameters used in EEZY, but Sinsabaugh et al. (2009) proposed that this consistent, nearly 1:1 ratio of enzymatic activities represents an equilibrium between the elemental composition of

microbial biomass and organic matter, given the efficiencies of microbial nutrient assimilation and growth. When we plotted the ratio of simulated $(dC_2/dt)/(dC_1/dt)$ versus dC_2/dt (Fig. 5b), it provided a pattern of relative turnover rates in C vs N-containing substrates by EEZY that closely matched the ratios of enzyme activities for ln(ßG)/ln(NAG + LAP) versus ln(ßG)/ln(acid phosphatase) shown by Sinsabaugh et al. (2009). This relationship is a roughly hyperbolic curve with one leg pointed towards the origin, demonstrating the effects of N-limitation, an inflection at the 1:1 ratio, and the second leg pointing straight up, reflecting C-limitations. Recently, Manzoni et al. (2010) noted that litter qualities converged during decomposition as nutrients were immobilized in relatively narrow ratios and excess elements were mineralized (including carbon). Sinsabaugh et al. (2009, 2010) showed that patterns of extracellular enzyme activity converged along with the qualities of residual organic matter. Thus observed patterns of extracellular enzyme activity and litter chemistry also appear to converge with progressive decomposition, and EEZY provides a mechanistic framework to interpret these interactions.

Finally, Sinsabaugh et al. (2008) found that the amount of soil organic matter (SOM) present had little impact on EEA_{CN}. The relationships, ln(ßG)/ln(SOM) and ln(NAG)/ln(SOM), had slopes of 0.98 ($R^2 = 0.55$) and 1.13 ($R^2 = 0.49$), respectively, over nearly two orders of magnitude in SOM content. Also, the ln(ßG)/ln(NAG) relationship had a slope of 1.02, similar to the relationships reported by Sinsabaugh et al. (2009, 2010). These results suggested that quality, rather than quantity of organic matter, controlled extracellular enzyme activity. Because EEZY estimates decay as an enzyme-saturated function α also shows no explicit response to substrate quantity. Hence our conceptually simple model of enzyme-mediated decomposition produced patterns of litter decay, extracellular enzyme activities and their responses to litter chemistry, microbial characteristics and enzyme kinetics that were consistent with extensive field observations.

4.3. Key model assumptions

EEZY is robust with respect to variations in key model parameters because the core equations calculating decomposition (Eqs. (1)–(3)) stabilize the relationships between soil organic matter, enzyme and biomass pool sizes. However, other models do not share some of these underlying assumptions, which if changed, would affect EEZY dynamics. Of these assumptions, possibly the most important is the relationship between CUE and CN_M. We used a fixed value of CN_M and assumed that excess C was lost through overflow metabolism. Without some mechanism for managing excess C, simulated decomposition would be inhibited in EEZY when $CN_1 > CN_M/CUE$. However, CN_M can vary for several reasons, such as changes in cellular constituents or community composition. A flexible CN_M could allow microorganisms to increase use of N-poor substrates without respiring as much of the extra C. There would still be a TER_{CN} defined by the upper limits to CN_M, and an optimum set of conditions where biomass and enzyme pools peak, and decomposition is maximal, but these peaks would extend over a larger range of CN_S. Of course, adding a flexible CN_M would require more parameters and assumptions regarding its controls. However, much of the apparently "excess" carbon in decomposition models (including some EEZY simulations) could be an artifact produced by combining various substrate pools. Although plant litter commonly has a high C:N ratio, most N exists in compounds like proteins and chitin, which are N-rich (Sterner and Elser, 2002) and would not generate excess C during decomposition.

We also viewed CUE as equivalent to growth efficiency for both biomass and enzymes, which does not include maintenance (R_M) or overflow (R_O) respiration. Unfortunately, CUE is a somewhat ambiguous term. Doi et al. (2010) defined the term, GE_C, with respect to TER_{CN}, GE_N and CN_M (Eq. (4)), that would necessarily include both R_M and R_O. Recently, Dijkstra et al. (2011) similarly defined CUE as simply the proportion of substrate that is incorporated into biomass, which also included R_M. However, most decomposition models define CUE as growth efficiency for routing C flow into biomass and calculate R_M as a separate characteristic of standing biomass (e.g., Parnas, 1976; Parton et al., 1987; Schimel and Weintraub, 2003; Moorhead and Sinsabaugh, 2006; Allison et al., 2010). This rationale is mathematically tractable and makes possible the exact, analytical solution for α used in EEZY. Including R_M in CUE would make CUE a function of decomposition and preclude this solution. Alternative formulations relating microbial growth to maintenance respiration have been explored (Beeftink et al., 1990; Van Bodegom, 2007), but also introduce more assumptions and model parameters. Analyses indicated that the biggest differences between these approaches occur when microorganisms are starved (Van Bodegom, 2007), not the case in any of our simulations.

Another key assumption was that microorganisms seek to balance their C and N requirements but this ignores other considerations that may influence substrate preference. For example, if the C from an N-containing substrate had higher assimilation efficiency than C from a C-only substrate, microorganisms could make more efficient use of C by preferentially utilizing the C–N substrate, which would increase N-mineralization. This effect is seen in planktonic communities where amino acid consumption can support a large fraction of production (Bradley et al., 2010; Sundback et al., 2011) and might explain why N-mineralization is reported when CN_S exceeds TER_{CN} (Doi et al., 2010; Sinsabaugh and Shah, 2011). This change could easily be incorporated in EEZY, by defining C preference according to assimilation efficiency, but it would require that substrate-specific efficiencies be known.

4.4. Future directions

A sensitivity analysis of EEZY showed that variations in enzyme kinetics had significant impacts on model behavior, suggesting the potential of this approach to evaluating effects of environmental factors on decomposition through their direct effects on enzyme activities. For example, the inhibitory effects of lignin on litter decay is well known (e.g., Melillo et al., 1982; Herman et al., 2008), and variously included in decomposition models (Meentemeyer, 1978; Parton et al., 1987; Moorhead and Sinsabaugh, 2006). Sinsabaugh (2010) showed that oxidase enzyme activities, which are responsible for the degradation of recalcitrant compounds, including lignin, were negatively related to soil organic matter content across ecosystems. Recently, Sinsabaugh and Shah (2011) showed that EEA_{CN} varied with the recalcitrance of organic matter, which they also related to oxidase activities. To date, we are aware of only one model that has simulated the effects of lignin concentration on the activity of extracellular enzymes responsible for decomposition (Sinsabaugh and Moorhead, 1995), but EEZY provides a context for more explicitly examining such enzyme-specific controls.

Acknowledgements

This work was supported by the USDA National Institute of Food and Agriculture Competitive Grant no. 2005-35107-16281; NSF Ecosystems Program grants DEB-0946257 and DEB-0918718; and the Environment and Agronomy Division of INRA. We also thank two anonymous reviewers whose suggestions greatly improved this work.

Appendix A. Model equations

The value of α represents the proportion of the total enzyme pool allocated to E_{C1}, and was determined by substituting Eqs. (1) and (2) for dC_1/dt and dC_2/dt in Eq. (3):

$$CN_M = CUE\cdot((k_d\cdot\alpha\cdot E_{CT}/(K+\alpha\cdot E_{CT}))+(k_d\cdot(1-\alpha)\cdot E_{CT}/(K+(1-\alpha)\cdot E_{CT})))/((k_d\cdot\alpha\cdot E_{CT}/(K+\alpha\cdot E_{CT}))/CN_1) \quad (A1)$$

This equation was reorganized to isolate α (Maplesoft v14, Waterloo Maple Inc.):

$$\alpha = 1/2\cdot\Big(2\cdot CUE\cdot CN_1\cdot E_{CT} - CN_M\cdot K - CN_M\cdot E_{CT} + \Big(4\cdot CUE^2\cdot CN_1^2\cdot E_{CT}^2 - 8\cdot CUE\cdot CN_1\cdot E_{CT}\cdot CN_M\cdot K - 4\cdot CUE\cdot CN_1\cdot E_{CT}^2\cdot CN_M + CN_M^2\cdot K^2 + 2\cdot CN_M^2\cdot K\cdot E_{CT} + CN_M^2\cdot E_{CT}^2 + 8\cdot CUE^2\cdot CN_1^2\cdot K\cdot E_{CT}\Big)^{1/2}\Big)\Big/E_{CT}/(2\cdot CUE\cdot CN_1 - CN_M) \quad (A2)$$

It is unlikely that values of CUE, k_d and K are the same for both substrates and both enzymes. For this reason, we wished to evaluate the effects of differences in these parameters and so assigned unique values of k_d and CUE for each of the two substrates and unique values of K for each of the two enzymes in Eqs. (1) and (2):

$$CN_M = (CUE_1\cdot k_{d1}\cdot\alpha\cdot E_{CT}/(K_1+\alpha\cdot E_{CT}) + CUE_2\cdot k_{d2}\cdot(1-\alpha)\cdot E_{CT}/(K_2+(1-\alpha)\cdot E_{CT}))/\times((k_{d1}\cdot\alpha\cdot E_{CT}/(K_1+\alpha\cdot E_{CT})/CN_1)) \quad (A3)$$

and again reorganized this equation to isolate α:

$$\alpha = 1/2\cdot\Big(k_{d2}\cdot CN_1\cdot CUE_2\cdot E_{CT} - k_{d2}\cdot CN_1\cdot CUE_2\cdot K_1 - k_{d1}\cdot CN_M\cdot K_2 + k_{d1}\cdot CN_1\cdot CUE_1\cdot K_2 + k_{d1}\cdot CN_1\cdot CUE_1\cdot E_{CT} - k_{d1}\cdot CN_M\cdot E_{CT} + \Big(-2\cdot k_{d2}\cdot CN_1\cdot CUE_2\cdot E_{CT}\cdot k_{d1}\cdot CN_M\cdot K_2 + 2\cdot k_{d2}\cdot CN_1^2\cdot CUE_2\cdot E_{CT}\cdot k_{d1}\cdot CUE_1\cdot K_2 + 2\cdot k_{d2}\cdot CN_1\cdot CUE_2\cdot K_1\cdot k_{d1}\cdot CN_M\cdot K_2 - 2\cdot k_{d2}\cdot CN_1^2\cdot CUE_2\cdot K_1\cdot k_{d1}\cdot CUE_1\cdot K_1 + 2\cdot k_{d2}\cdot CN_1^2\cdot CUE_2\cdot K_1\cdot k_{d1}\cdot CUE_1\cdot E_{CT} - 2\cdot k_{d2}\cdot CN_1\cdot CUE_2\cdot + K_1\cdot k_{d1}\cdot CN_M\cdot E_{CT} + k_{d1}^2\cdot CN_M^2\cdot K_2^2 + k_{d1}^2\cdot CN_M^2 + 2\cdot k_{d2}\cdot CN_1^2\cdot CUE_2\cdot E_{CT}^2\cdot k_{d1}\cdot CUE_1 - 2\cdot k_{d2}\cdot CN_1\cdot CUE_2\cdot E_{CT}^2\cdot k_{d1}\cdot CN_M - 4\cdot k_{d1}^2\cdot CN_M\cdot K_2\cdot CN_1\cdot CUE_1\cdot E_{CT} + 2\cdot k_{d2}^2\cdot CN_1^2\cdot CUE_2^2\cdot E_{CT}\cdot K_1 - 2\cdot k_{d1}^2\cdot CN_M\cdot K_2^2\cdot CN_1\cdot CUE_1 + 2\cdot k_{d1}^2\cdot CN_1^2\cdot CUE_1^2\cdot K_2\cdot E_{CT} - 2\cdot k_{d1}^2\cdot CN_1\cdot CUE_1\cdot E_{CT}^2\cdot CN_M + k_{d2}^2\cdot CN_1^2\cdot CUE_2^2\cdot E_{CT}^2 + k_{d2}^2\cdot CN_1^2\cdot CUE_2^2\cdot K_1^2 + 2\cdot k_{d1}^2\cdot CN_M^2\cdot K_2\cdot E_{CT} + k_{d1}^2\cdot CN_1^2\cdot CUE_1^2\cdot K_2^2 + k_{d1}^2\cdot CN_1^2\cdot CUE_1^2\cdot E_{CT}^2\Big)^{1/2}\Big)\Big/E_{CT}/(k_{d1}\cdot CN_1\cdot CUE_1 + k_{d2}\cdot CN_1\cdot CUE_2 - k_{d1}\cdot CN_M) \quad (A4)$$

Both equations (Eqs. (A2) and (A4)) provided exact solutions for α. This value was compared to the existing sizes of the two enzyme pools, and new enzyme production was allocated to meet α. Eq. (A4) collapses to Eq. (A2) when $k_{d1}=k_{d2}$, $K_1=K_2$ and $CUE_1=CUE_2$. Note that our allocation scheme did not explicitly include maintenance respiration (R_M). This omission assumes that microbial resource demand places priority on production, a simplifying assumption that was tested and confirmed by Schimel and Weintraub (2003). All C released by decomposition of both substrate pools entered the DOC pool. Nitrogen released from C_1 decomposition (N_1) balanced C release:

$$dN_1/dt = -dC_1/dt\cdot CN_1 \quad (A5)$$

and was added to the DON pool. All materials in the DOC and DON pools were fully utilized each day. The first priority was enzyme production, which was a fraction (K_E) of the most limiting resource, i.e., either DON or DOC. Enzymes also had a constant turnover rate (K_N). Thus the enzyme C-pool dynamics were estimated:

$$dE_{CT}/dt = K_E\cdot\min(DOC, DON/CN_E) - K_N\cdot E_{CT} \quad (A6)$$

Enzyme N dynamics balanced C flows:

$$dE_{NT}/dt = CN_E\cdot dE_{CT}/dt \quad (A7)$$

Respiration associated with enzyme production (R_E) was calculated as a fraction (CUE) of this production:

$$R_E = K_E\cdot\min(DOC, DON/CN_E)\cdot(1-CUE)/CUE \quad (A8)$$

Maintenance respiration (R_M) of microorganisms was estimated as a fraction (K_M) of standing biomass:

$$R_M = K_M\cdot B_C \quad (A9)$$

Microbial growth was calculated as a fraction (CUE) of the most limiting resource minus the allocation to enzyme production, R_E, and R_M. Biomass had a constant turnover (K_T):

$$dB_C/dt = CUE\cdot(1-K_E/CUE)\cdot(\min(DOC, DON/CN_M) - R_M) - K_T\cdot B_C \quad (A10)$$

Biomass N dynamics balanced C flows:

$$dB_N/dt = CN_M\cdot dB_N/dt \quad (A11)$$

Respiration associated with biomass growth (R_G) was calculated as a fraction (CUE) of this production:

$$R_G = (1-CUE)\cdot(1-K_E/CUE)\cdot(\min(DOC, DON/CN_M) - R_M) \quad (A12)$$

Any carbon released from soil organic matter in excess of requirements for biomass growth and enzyme production was assumed lost via overflow metabolism (R_O):

$$R_O = DOC - K_E\cdot\min(DOC, DON/CN_E)/CUE - (1-K_E/CUE)\cdot(\min(DOC, DON/CN_M) - R_M) \quad (A13)$$

If the decomposition of C_1 released more N from N_1 to the DON pool than was needed to meet the needs for microbial growth and enzyme production, the excess was mineralized.

$$M_m = DOC - CN_E\cdot K_E\cdot\min(DOC, DON/CN_E) - CN_M\cdot CUE\cdot(1-K_E/CUE)\cdot(\min(DOC, DON/CN_M) - R_M) \quad (A14)$$

For the sake of simplicity, we did not include the immobilization of mineral N into microbial biomass, and thus the potential effects of N immobilization on enzyme allocation.

References

Allen, A.P., Gillooly, J.F., 2009. Towards an integration of ecological stoichiometry and the metabolic theory of ecology to better understand nutrient cycling. Ecology Letters 12, 369–384.

Allison, S.D., 2005. Cheaters, diffusion and nutrients constrain decomposition by microbial enzymes in spatially structured environments. Ecology Letters 8, 626–635.

Allison, S.D., Wallenstein, M.D., Bradford, M.A., 2010. Soil-carbon response to warming dependent on microbial physiology. Nature Geoscience 3, 336–340.

Beeftink, H., Van der Heijden, R., Heijnen, J., 1990. Maintenance requirements: energy supply from simultaneous endogenous respiration and substrate consumption. FEMS Microbiology Letters 73, 203–209.

Bradley, P.B., Lomas, M.W., Bronk, D.A., 2010. Inorganic and organic nitrogen use by phytoplankton along Chesapeake Bay, measured using a flow cytometric sorting approach. Estuaries and Coasts 33, 971–984.

Brown, J.H., Gillooly, J.F., Allen, A.P., Savage, V.M., West, G.B., 2004. Toward a metabolic theory of ecology. Ecology 85, 1771–1789.

Burns, R.G., Dick, R.P., 2002. Enzymes in the Environment: Activity, Ecology, and Applications. Marcel Dekker, New York.

Burns, R.G., 1978. Soil Enzymes. Academic Press, New York.

Davidson, E.A., Samanta, S., Caramori, S.S., Savage, K., 2012. The Dual Arrhenius and Michaelis–Menten kinetics model for decomposition of soil organic matter at hourly to seasonal time scales. Global Change Biology 18, 371–384.

Dijkstra, P., Thomas, S.C., Heinrich, P.L., Koch, G.W., Schwartz, E., Hungate, B.A., 2011. Effect of temperature on metabolic activity of intact microbial communities: evidence for altered metabolic pathway activity but not for increased maintenance respiration and reduced carbon use efficiency. Soil Biology & Biochemistry 43, 2023–2031.

Doi, H., Cherif, M., Iwabuchi, T., Katano, I., Stegen, J.C., Striebel, M., 2010. Integrating elements and energy through the metabolic dependencies of gross growth efficiency and the threshold elemental ratio. Oikos 119, 752–765.

Frost, P.C., Benstead, J.P., Cross, W.F., Hillebrand, H., Larson, J.H., Xenopoulos, M.A., Yoshida, T., 2006. Threshold elemental ratios of carbon and phosphorus in aquatic consumers. Ecology Letters 9, 774–779.

Herman, J., Moorhead, D., Berg, B., 2008. The relationship between rates of lignin and cellulose decay in aboveground forest litter. Soil Biology & Biochemistry 40, 2620–2626.

Manzoni, S., Porporato, A., 2009. Soil carbon and nitrogen mineralization: theory and models across scales. Soil Biology & Biochemistry 41, 1355–1379.

Manzoni, S., Trofymow, J.A., Jackson, R.B., Porporato, A., 2010. Stoichiometric controls on carbon, nitrogen, and phosphorus dynamics in decomposing litter. Ecological Monographs 80, 89–106.

Marklein, A.R., Houlton, B.Z., 2011. Nitrogen inputs accelerate phosphorus cycling rates across a wide variety of terrestrial ecosystems. New Phytologist 193, 696–704.

Marx, M.C., Wood, M., Jarvis, S.C., 2001. A microplate fluorimetric assay for the study of enzyme diversity in soils. Soil Biology & Biochemistry 33, 1633–1640.

Meentemeyer, V., 1978. Macroclimate and lignin control of litter decomposition rates. Ecology 59, 465–472.

Melillo, J.M., Aber, J.D., Muratore, J.F., 1982. Nitrogen and lignin control of hardwood leaf litter decomposition dynamics. Ecology 63, 621–626.

Moorhead, D.L., Sinsabaugh, R.L., 2006. A theoretical model of litter decay and microbial interaction. Ecological Monographs 67, 151–174.

Parnas, H., 1976. A theoretical explanation of the priming effect based on microbial growth with two limiting substrates. Soil Biology & Biochemistry 8, 139–144.

Parton, W.J., Schimel, D.S., Cole, C.V., Ojima, D.S., 1987. Analysis of factors controlling soil organic matter levels in Great Plains Grasslands. Soil Science Society of America Journal 51, 1173–1179.

Santos, L.O., Dewasme, L., Coutinho, D., Vande Wouwer, A., 2012. Nonlinear model predictive control of fed-batch cultures of micro-organisms exhibiting overflow metabolism: assessment and robustness. Computers and Chemical Engineering 39, 143–151.

Schultz, P., Urban, N.R., 2008. Effects of bacterial dynamics on organic matter decomposition and nutrient release from sediments. A modeling study. Ecological Modelling 210, 1–14.

Schimel, J.P., Weintraub, M.N., 2003. The implications of exoenzyme activity on microbial carbon and nitrogen limitation in soil: a theoretical model. Soil Biology & Biochemistry 35, 549–563.

Sinsabaugh, R.L., 1994. Enzymatic analysis of microbial pattern and Process. Biology and Fertility of Soils 17, 69–74.

Sinsabaugh, R.L., 2010. Phenol oxidase, peroxidase and organic matter dynamics of soil. Soil Biology & Biochemistry 42, 391–404.

Sinsabaugh, R.L., Findlay, S., Franchini, P., Fisher, D., 1997. Enzymatic analysis of riverine bacterioplankton production. Limnology and Oceanography 42, 29–38.

Sinsabaugh, R.L., Hill, B.H., Shah, J.J.F., 2009. Ecoenzymatic stoichiometry of microbial organic nutrient acquisition in soil and sediment. Nature 462, 795–797.

Sinsabaugh, R.L., Lauber, C.L., Weintraub, M.N., Ahmed, B., Allison, S.D., Crenshaw, C., Contosta, A.R., Cusack, D., Frey, S., Gallo, M.E., Gartner, T.B., Hobbie, S.E., Holland, K., Keeler, B.L., Powers, J.S., Stursova, M., Takacs-Vesbach, C., Waldrop, M.P., Wallenstein, M.D., Zak, D.R., Zeglin, L.H., 2008. Stoichiometry of soil enzyme activity at global scale. Ecology Letters 11, 1252–1264.

Sinsabaugh, R.L., Moorhead, D.L., 1994. Resource-allocation to extracellular enzyme production – a model for nitrogen and phosphorus control of litter decomposition. Soil Biology & Biochemistry 26, 1305–1311.

Sinsabaugh, R.L., Moorhead, D.L., 1995. Synthesis of litter quality and enzymic approaches to decomposition modeling. In: Cadisch, G., Giller, K.E. (Eds.), Driven by Nature: Plant Litter Quality and Decomposition. CAB International, Cambridge, pp. 363–375.

Sinsabaugh, R.L., Shah, J.J.F., 2011. Ecoenzymatic stoichiometry of recalcitrant organic matter decomposition: the growth rate hypothesis in reverse. Biogeochemistry 102, 31–43.

Sinsabaugh, R.L., Shah, J.J.F., Hill, B.H., Elonen, C.M., 2011. Ecoenzymatic stoichiometry of stream sediments with comparison to terrestrial soils. Biogeochemistry. doi:10.1007/s10533-011-9676-x.

Sinsabaugh, R.L., Van Horn, D.J., Shah, J.J.F., Findlay, S., 2010. Ecoenzymatic stoichiometry in relation to productivity for freshwater biofilm and plankton communities. Microbial Ecology 60, 885–893.

Sterner, R.W., Elser, J.J., 2002. Ecological Stoichiometry: The Biology of Elements from Molecules to the Biosphere. Princeton University, Princeton.

Sundback, K., Lindehoff, E., Graneli, E., 2011. Dissolved organic nitrogen: an important source of nitrogen for the microphytobenthos in sandy sediment. Aquatic Microbial Ecology 63, 89–100.

Van Bodegom, P., 2007. Microbial maintenance: a critical review on its quantification. Microbial Ecology 53, 513–523.